ESTIMATION OF MATRIX BLOCK SIZE DISTRIBUTION IN NATURALLY FRACTURED RESERVOIRS

A Report Submitted to the Department of Petroleum Engineering of Stanford University in Partial Fulfillment of the Requirements for the Degree of Master of Science.

by
Ashok Kumar Belani
August 1988

Contents

1 ACKNOWLEDGEMENTS

I sincerely thank my research advisor, Y. Jalali-Yazdi for his able guidance and patient help during the course of this research work and during the preparation of the Report. I have enjoyed working with him.

I thank also the Faculty, students and staff of the Petroleum Engineering department for the numerous discussions I had on subjects related to the study.

Finally, I thank Schlumberger for having provided partial support for my Master's program at Stanford.

2 ABSTRACT

Interporosity flow in a naturally fractured reservoir is modelled by a new formulation incorporating variability in matrix block size. Matrix block size is inversely related to fracture intensity. The size of matrix elements contributing to interporosity flow is expressed as a distribution in the source term of the diffusivity equation. The pressure transient response for uniform and bimodal distributions of block size is investigated. Both pseudo-steady state and transient models of flow are analysed. It is shown that features observed on the pressure derivative curve can yield the parameters of the distribution. Thus, observed pressure response from fractured reservoirs can be analysed to obtain the matrix block size distribution in the volume of the reservoir investigated by the test.

The solution to the uniform distribution can be extended to more general distributions. Other sources of information, like logs and geological observations, can give an estimation of the shape of the distribution, and this model can be used to compute the reservoir parameters.

3 INTRODUCTION

Flow tests in naturally fractured reservoirs have been analysed using a continuum approach to model the reservoir, i.e., matrix and fracture systems are assumed continuous throughout the formation.[1,2] The rock matrix has a very low permeability but stores most of the reservoir fluid in its intergranular porosity. The fracture system, on the other hand, has an extremely low porosity but provides the path of principal permeability.

When a well located in such a reservoir is produced, a rapid pressure response occurs in the fracture network due to its high diffusivity. This creates a pressure difference between the matrix and the fractures, which begins to deplete the fluid from the matrix, commonly termed as interporosity flow. As flow progresses, pressures in the matrix and the fractures equilibrate and the fracture flow response is observed again, with fluid now coming from a composite storativity of the matrix and the fractures.

The interaction between the matrix and the fractures is affected strongly by the geometrical distribution of the fractures. The parameters used to characterise this interaction are ω_m, matrix storativity ratio, which specifies the relative fluid distribution, and X, the interporosity flow coefficient, which lumps the effects of the flow properties of both media and their geometry. Matrix flow can be modelled as pseudo-steady state (PSS),[3] or unsteady state (USS).[4,5]

Models available in the literature assume fracturing is uniform and hence matrix block size is constant. Geologic studies have shown nonuniformity in fracture intensity in many reservoirs, from very severe fracturing to very sparse fractures.[6-9] Hence, it is necessary to model variability in flow contribution from matrix elements or blocks, depending on their size.

The evolution of the double porosity model is explained in the next section.

This work is the development of a robust and general fractured reservoir model allowing any distribution of matrix block size. Matrix block size distibution affects the pressure response significantly. The sensitivity of the pressure response is studied for the uniform and bimodal distributions and parameter estimation is discussed.

4 LITERATURE REVIEW

The double porosity concept was introduced in 1960 by Barenblatt et al.[1,2] As explained before, it assumed the existence of two porous regions of distinctly different porosities and permeabilities within the formation. Also, a continuum was assumed, where any small volume contained a large proportion of both media. Hence each point in space had associated with it two pressure values, P_f in the permeable medium and P_m in the porous, less permeable medium. Interporosity flow was assumed to occur in pseudo-steady state condition,

$$q = \frac{\lambda}{\mu} k_m (P_m - P_f).$$

The solution was completed in 1963 by Warren and Root[3] who described the reservoir geometry as an orthogonal system of continuous, uniform fractures, each parallel to the principle axis of permeability. Two parameters were defined to characterize the double porosity behaviour :

- The inter-porosity flow coefficient:

  $$\lambda = \alpha \frac{k_m}{k_f} r_w^2,$$

  where k_f is the fracture permeability, r_w the wellbore radius and α a geometrical factor with dimensions of reciprocal area.

- The fracture storativity:

  $$\omega_f = \frac{\phi_f c_f}{\phi_f c_f + \phi_m c_m},$$

  where ϕ_f is the fracture porosity, ϕ_m the matrix porosity and C_f and C_m the corresponding fluid compressibilities.

Pseudo-steady state flow was assumed for the matrix as a suitable approximation for late time data. The results were analysed on semilog plots, characterizing the interporosity flow region for different values of λ and w.

$$\overline{P}_{D_w} = \frac{K_0(x)}{sxK_1(x)},$$

where $x = \sqrt{sf(s)}$, and

$$f(s) = \frac{\omega(1-\omega)s+\lambda}{(1-\omega)s+\lambda}.$$

Odeh[15] suggested in 1965 that wellbore storage effects dominated pressure response at early times, and hence the first straight line may not be observed.

Kazemi[16] (1969) and De Swaan[17] (1976) removed the pseudo-steady state assumption and numerically solved the transient problem for flow from marix to fractures. Kazemi also considered flow directly from the matrix to the wellbore and concluded that the results showed insignificant difference.

Kazemi also applied the solution to interference tests, solving the equation both analytically and numerically.

Mavor and Cinco[18] added wellbore storage and skin to the pseudo-steady state flow solution of Warren and Root.

In 1980, Najurieta[19] proposed an approximate solution for the equation presented by De Swaan. The time domain approximation was of the same form as the homogeneous reservoir solution. It presented a way to group parameters to facilitate the solution of the inverse problem.

Type curves for analysing wells with wellbore storage and skin in double porosity reservoirs were introduced by Bourdet and Gringarten.[20] It was claimed that even in the absence of the first straight line on the semi-log plot, a log-log type curve analysis could yield all reservoir parameters. Dimensionless parameters were defined. The idea of computing fissure volume and matrix block size was presented but was not convincing.

A major contribution was made by Bourdet et al[21,22] in 1983 when the pressure derivative plot was introduced as a tool to analyse pressure test data. The inter-porosity flow region was identified as a distinct feature and could be characterized by the λ and the ω parameters. Both pseudo steady state and the transient matrix flow models could be analysed.

At the same time, Streltsova[23] showed that the transient flow in the matrix did not cause an inflection point on the pressure profile on the

semilog plot. A transition straight line was proposed with a slope equal to one half the slope of the early or late time straight lines. This facilitated a Horner plot analysis.

All models presented thus far assumed the orthogonal system of uniform, continuous fractures, as proposed by Warren and Root. Matrix blocks in between the fractures were of the same size and shape.

Numerous studies in geology and well logging have shown the existence of nonuniformly fractured reservoirs. The Warren and Root model is an over-simplification of reality. There is need to develop a model which honors the heterogeneity in matrix block properties. Since the matrix-fracture interface area is dependent on the geometry of the matrix blocks, a distribution of matrix block geometries must be considered. The shape of the blocks does not have a significant effect on the response and hence a variability in block size shall be considered in this work.

Braester[10] concluded block size does not significantly affect the drawdown pressure response of a fractured reservoir. Cinco et al[11] suggested a discrete distribution of matrix block sizes with transient interporosity flow and showed the pressure derivative is significantly affected. Jalali-Yazdi and Belani[12] show block size variability affects the pressure response markedly.

It would be more appropriate to lump all flow criteria into the flow coefficient X and consider a distribution of matrix elements with different flow coefficients. The engineering concept of matrix blocks would be replaced by that of matrix volume elements with a variability in their contribution to interporosity flow. This idea has many strengths in modelling the reservoir and understanding its flow behaviour, and hence will be the subject of later research.

5 MODEL FORMULATION

The classical development of the diffusivity equation from mass balance in a fracture element yields :

$$\frac{1}{r}\frac{\partial}{\partial r}\left(r\frac{\partial P_f}{\partial r}\right) = \frac{\phi_f c_f \mu}{k_f}\frac{\partial P_f}{\partial t} + Q_m, \tag{1}$$

where P_f is the pressure in the fracture and Q_m is the interporosity flow source term. Eqn.(1) assumes:

- radial, cylindrical flow occurs in the fracture,
- reservoir fluid is slightly compressible and has constant properties,
- inertial and gravity effects can be ignored and Darcy's law is applicable, and
- rock properties are constant.

Formulation of the flow contribution term Q_m requires a reservoir model, since the geometrical distribution of the fractures governs interporosity flow. In a uniformly fractured reservoir where block size is constant, the flow contribution from a single block into the adjoining fracture depends upon the storativity, permeability, and the size of the block. Such models have been presented in the literature.[1-5] In a nonuniformly fractured reservoir with a random distribution of matrix block size (Figs. 1,2), the matrix contribution is :

$$Q_m = \int_{h_{min}}^{h_{max}} Q(h) f(h) dh, \tag{2}$$

where Q(h) is the flow contribution from a block of size h and f(h) is the probability of occurrence of block size h. The flow contribution Q(h) is specified by the mode of interporosity flow and the shape of the matrix block.

Note for a constant block size model, matrix block size distribution f(h) is a shifted Dirac delta function δ(h-H):

$$Q_m = \int_{h_{min}}^{h_{max}} \delta(h - H) Q(h) dh = Q(H), \tag{3}$$

which is consistent with the Warren and Root[3] and other single block size models.[4,5]

For reservoirs with intense fracturing, f(h) is a positively skewed distribution 'favoring' small blocks, and for reservoirs with sparse fracturing, f(h) is a negatively skewed distribution, 'favoring' large blocks.

A more general formulation of the source integral can account for variability in several matrix properties. For instance, a random variation in block permeability k_m and block size h, results in :

$$Q_m = \int_{h_{min}}^{h_{max}} \int_{k_{min}}^{k_{max}} Q(k_m, h) f(k_m, h) dk_m dh, \qquad (4)$$

where $Q(k_m,h)$ is the flow contribution from a block of size h and permeability k_m and $f(k_m,h)$ is a joint probability distribution. This work addresses variability in matrix block size only and hence Eqn.(4) is not further pursued.

6 SOLUTION

Equations **(1)** and **(2)** are solved for slab matrix blocks for the initial and boundary conditions stated in the Appendix. The wellbore pressure response in the Laplace space **is:**

$$\overline{P}_{D_w} = \frac{K_0(x) + S_D x K_1(x)}{s[C_D s(K_0(x) + S_D x K_1(x)) + x K_1(x)]}, \tag{5}$$

where s is the Laplace variable related to dimensionless time:

$$t_D = \frac{k_f t}{(\phi_f c_f + \phi_m c_m)\mu r_w^2}, \tag{6}$$

and the argument $x = \sqrt{sg(s)}$.
For PSS:

$$g(s) = \omega_f + \omega_m \int_{\frac{h_{min}}{h_{max}}}^{1} \frac{3\lambda}{\omega_m s + 3\lambda} f(h_D) dh_D. \tag{7}$$

For USS:

$$g(s) = \omega_f + \int_{\frac{h_{min}}{h_{max}}}^{1} \sqrt{\frac{\omega_m \lambda}{s}} \tanh\left(\sqrt{\frac{\omega_m s}{\lambda}}\right) f(h_D) dh_D. \tag{8}$$

The dimensionless parameters are defined below :

$$P_{D_f} = \frac{2\pi k_f h_f}{q\mu B}(P_i - P_f), \tag{9}$$

$$P_{D_m} = \frac{2\pi k_f h_f}{q\mu B}(P_i - P_m), \tag{10}$$

$$\omega_m = \frac{\phi_m c_m}{(\phi_m c_m + \phi_f c_f)}, \tag{11}$$

$$\omega_f = \frac{\phi_f c_f}{(\phi_m c_m + \phi_f c_f)}, \tag{12}$$

$$\lambda = \frac{k_m r_w^2}{k_f h^2}, \tag{13}$$

$$r_D = \frac{r}{r_w} \tag{14}$$

$$\xi_D = \frac{\xi}{h} \tag{15}$$

$$h_D = \frac{h}{h_{max}} \tag{16}$$

The interporosity **flow** coefficient λ depends on h and hence is included in the integral in Eqns. (7) and (8); these equations collapse to the single block size case if $f(h_D)$ is **a** Dirac delta function.

The pressure response is markedly governed by the distribution function in Eqns.(7) and **(8).** Geologic studies of outcrops do not express observed fracture intensities in terms of block size, hence it is difficult to choose any particular shape of block size distribution. This **work** solves the cases of Uniform and Bimodal distributions.

7 UNIFORM DISTRIBUTION

A distribution of interest is the uniform or rectangular distribution where all block sizes (h_{min} to h_{max}) have an equal chance of occurrence:

$$f(h) = \frac{1}{h_{max} - h_{min}}, \tag{17}$$

with mean block size:

$$h_{mean} = \frac{h_{min} + h_{max}}{2}, \tag{18}$$

and variance:

$$\sigma_h^2 = \frac{1}{12}(h_{max} - h_{min})^2. \tag{19}$$

The applicability of the uniform distribution is two-fold:

1. It should be used when the matrix block size distribution is unknown.
2. A sum of uniform distributions of small variance spread can approximate any distribution and hence the pressure response for other distributions can be obtained.

For PSS flow, Eqns. (7), (12)-(14) yield:

$$g(s) = \omega_f + \omega_m \frac{\sqrt{3\lambda_{min}/\omega_m s}}{1-\sqrt{\lambda_{min}/\lambda_{max}}} \times$$

$$(tan^{-1}\sqrt{3\lambda_{max}/\omega_m s} - tan^{-1}\sqrt{3\lambda_{min}/\omega_m s}). \tag{20}$$

For USS flow, Eqns. (8), (12)-(14) yield:

$$g(s) = \omega_f + \frac{\omega_m \sqrt{\lambda_{min}/\omega_m s}}{2(1-\sqrt{\lambda_{min}/\lambda_{max}})} \times$$

$$\int_{\lambda_{min}}^{\lambda_{max}} \frac{1}{\lambda} \tanh \sqrt{\frac{\omega_m s}{\lambda}} d\lambda. \tag{21}$$

Eqn. (18) does not have a closed form analytical solution and requires numerical integration.

The block sizes h_{min} and h_{max} correspond to interporosity flow coefficients λ_{max} and λ_{min}, respectively:

$$\frac{\lambda_{min}}{\lambda_{max}} = (\frac{h_{min}}{h_{max}})^2. \tag{22}$$

The $\lambda_{max}/\lambda_{min}$ ratio governs the variance of the uniform distribution. As this ratio approaches unity, the uniform distribution approaches a Dirac delta function and hence the pressure response approaches the single block size response.

8 BIMODAL DISTRIBUTION

General tectonic stresses over a region can cause fracturing at a **macro** scale and associated breaking of the rock at **a** finer scale. **This** results in two controlling sets of matrix block sizes, which can be represented by a bimodal distribution. If the two modes **of** the distribution are equally probable (same height), then:

$$f(h_D) = \frac{1}{1 - \frac{h_1}{h_{max}} + \frac{h_2}{h_{max}} - \frac{h_3}{h_{max}}}, \tag{23}$$

where $h_1 < h_2 < h_3 < h_{max}$ correspond to $\lambda_1 > \lambda_2 > \lambda_3 > \lambda_{min}$, respectively. The **PSS** solution for this distribution function **is:**

$$g(s) = \omega_f + \frac{\omega_m}{1 - \sqrt{\frac{\lambda_{min}}{\lambda_1}} + \sqrt{\frac{\lambda_{min}}{\lambda_2}} - \sqrt{\frac{\lambda_{min}}{\lambda_3}}} \sqrt{\frac{3\lambda_{min}}{\omega_m s}} \times$$

$$(tan^{-1}\sqrt{\frac{3\lambda_1}{\omega_m s}} - tan^{-1}\sqrt{\frac{3\lambda_2}{\omega_m s}} + tan^{-1}\sqrt{\frac{3\lambda_3}{\omega_m s}} - tan^{-1}\sqrt{\frac{3\lambda_{min}}{\omega_m s}}). \tag{24}$$

9 DISCUSSICN

Figure (3) shows the **PSS** pressure and pressure derivative response for uniform block size distributions of different variance spread (X ratio). X is kept constant at 10^{-5} and λ_{min} varies from 10^{-5} to 10^{-9} by an order of magnitude at each step. Figure 3 indicates:

1. In the limit λ_{min} approaches λ_{max} (or vice versa), the single block size response is obtained (Warren and Root[3]).

2. The interporosity flow region on the derivative curve shows distinctly the effect of the variation in block size. The contribution from each block size affects the pressure at a different point in time depending on the interporosity flow coefficient, causing a stretching of the derivative curve. The change from the characteristic 'peaked valley' to a stretched valley with more features, is hence dependent on the block size distribution.

3. The beginning of the late time semi-log straight line ($P'_D = 0.5$) is inversely related to λ_{min} (slowest contributing block), with an approximate relation:

$$T_{D_E} \approx \frac{1}{\lambda_{min}}. \tag{25}$$

The solution was investigated for other values of λ_{max}, varying X ratio. Figure (4) shows the pressure derivative response for, X of 10^{-4} and X ratios of 1to 10000. Similarly, Fig.(5) shows the response for λ_{max} of 10^{-6} and the same X ratio values. Identical derivative profiles are obtained for a given ω_m and X ratio; only the placement of the profile in time is governed by the magnitude of the flow coefficients.

Figure (6) illustrates the response for a range of matrix storativity (ω_m) for $\lambda_{max} = 10^{-5}$ and $\lambda_{min} = 10^{-7}$. The 'stretched' transition curve characterizes the variance of the distribution function as noted in Fig.(3). Also, $P'_{D_{min}}$ and T^*_D (the coordinates of the point of inflection) increase with decreasing ω.

The response was closely studied for the inflection points in the three cases of Figs. 3,4,5. The data is presented in Tables 1,2,3.

Figure (7) is a correlation of slope ratio (SR) and w, and $\lambda_{min}/\lambda_{max}$. SR is the ratio of semi-log slope at the point of inflection and the early time or late time semi-log slope, $SR = P'_{D_{min}}/0.5$.[13,14] SR is independent of the magnitude of λ_{min} and χ.

Figure (8) is a correlation of T_{D_E} and λ_{min} as indicated by Eqn.(22).

Figure (9) indicates the time at which the transition curve begins, T_{D_B}, is a dominant function of λ_{max} but also varies with the variance of the distribution function (χ ratio).

Figure (10) illustrates the time coordinate of the point of inflection, T^*_D, depends on the magnitude of the interporosity flow coefficients. However, the ratio T_{D_E}/T^*_D is a function of w, and χ ratio and not of the χ values.

Figure (11) illustrates the effect of wellbore storage on the pressure response. Flow tests where early time data may be lost should be run long enough to obtain T_{D_E}.

Figure (12) exhibits the pressure response for the unsteady state mode of interporosity flow. The χ distribution is the same as that of Fig.(3) but w, is 0.99. The features of Fig.(10) are similar to those of the pseudo-steady state response (Fig.3), although less pronounced.

The relations illustrated above can be used to estimate ω_m, λ_{min}, and χ from pressure transient data. Alternatively, use of the proposed solution (Eqns. 5,17,18) in nonlinear regression of pressure data yields the reservoir parameters.

Figures (13) and (14) illustrate the pressure response for a bimodal distribution with the parameters, $\lambda_1 = 10^{-5}$, $\lambda_2 = 0.8 \times 10^{-5}$, $\lambda_3 = 10^{-6}$ and $\lambda_{min} = 0.8 \times 10^{-6}$. Figure (15) exhibits the response for a bimodal distribution with $\lambda_1 = 10^{-5}$, $\lambda_2 = 0.8 \times 10^{-5}$, $\lambda_3 = 10^{-7}$ and $\lambda_{min} = 0.8 \times 10^{-7}$. Figures (16) and (17) exhibit the response for a bimodal distribution with $\lambda_1 = 10^{-5}$, $\lambda_2 = 0.8 \times 10^{-5}$, $\lambda_3 = 10^{-8}$ and $\lambda_{min} = 0.8 \times 10^{-8}$. Figure (18) exhibits the response for a bimodal distribution with $\lambda_1 = 10^{-5}$, $\lambda_2 = 0.8 \times 10^{-5}$, $\lambda_3 = 10^{-9}$ and $\lambda_{min} = 0.8 \times 10^{-9}$.

When the two modes of the distribution are very close, the response is similar to that of the unimodal uniform distribution corresponding to the larger χ mode. As the separation between the two modes increases, the pressure response deviates from that of the unimodal distribution. Beyond a certain degree of separation, the derivative plot character due to the higher χ mode is suppressed.

The solutions of the unimodal and bimodal distributions can be extended to multimodal distributions, which may be obtained from geologic information. The procedure would be *to* estimate a shape of the distribution from well-log data and compute the parameters using the pressure response.

10 CONCLUSIONS

1. A robust formulation of pressure transient response in nonuniformly fractured reservoirs is presented.
2. The matrix block size distribution for a uniformly fractured reservoir is a Dirac delta function and results in a sharp pressure response.
3. The pressure response of a nonuniformly fractured reservoir becomes less pronounced with an increase in the variance of the matrix block size distribution.
4. The pressure derivative curve for uniform distribution can be analysed to estimate the reservoir parameters.

11 NOMENCLATURE

B	=	formation volume factor, RB/STB
c	=	compressibility, psi^{-1}
c_f	=	fracture total compressibility, psi^{-1}
c_m	=	matrix total compressibility, psi^{-1}
C_D	=	wellbore storage coefficient, dimensionless
f(h)	=	block size distribution function, ft^{-1}
$f(h_D)$	=	block size distribution function, dimensionless
$f(k_m, h)$	=	joint probability distribution function, $ft^{-1}.md^{-1}$
g(s)	=	a parameter in the Bessel function argument
h	=	matrix block size variable, ft
h_D	=	matrix block size, dimensionless
h_f	=	fracture thickness, ft
h_{min}	=	minimum block size, uniform distribution, ft
h_{max}	=	maximum block size, uniform distribution, ft
h_{mean}	=	mean block size, uniform distribution, ft
h_1, h_2, h_3	=	block size bounds for bimodal distribution, ft
H	=	constant matrix block size, ft
k_f	=	fracture permeability, md
k_m	=	matrix permeability, md

$K_0(x)$	=	modified Bessel function, second kind, zero order
$K_1(x)$	=	modified Bessel function, second kind, first order
P_{D_f}	=	fracture pressure, dimensionless
P_{D_m}	=	matrix pressure, dimensionless
$\bar{P}_{D_w}$	=	Laplace transformed wellbore pressure response
P_f	=	fracture fluid pressure, psi
P_i	=	initial pressure, psi
P_m	=	matrix fluid pressure, psi
PSS	=	pseudo-steady state
q	=	volumetric flow rate, STB/D
Q(h)	=	flow contribution of matrix size h, *hour-'*
Q(k_m, h)	=	flow contribution of matrix size h and permeability k_m, *hour-'*
Q_m	=	cumulative matrix flow contribution, *hour''*
r	=	radial coordinate, ft
r_D	=	radial coordinate, dimensionless
r_w	=	wellbore radius, **ft**
s	=	Laplace parameter
S_D	=	skin factor, dimensionless
SR	=	minimum slope ratio, dimensionless
t	=	time, hours
t_D	=	time, dimensionless
T_{D_B}	=	time transition period begins, dimensionless
T_{D_E}	=	time transition period ends, dimensionless
T_D^*	=	time of minimum slope, dimensionless

USS	=	unsteady state
x	=	Bessel function argument
$\delta(h-H)$	=	Dirac delta function
λ	=	interporosity **flow** coefficient, dimensionless
$\lambda_1, \lambda_2, \lambda_3$	=	interporosity **flow** coefficients, bimodal distribution, dimensionless
λ_{max}	=	maximum interporosity **flow** coefficient, dimensionless
λ_{min}	=	minimum interporosity **flow** coefficient, dimensionless
μ	=	viscosity, cp
ξ	=	normal coordinate to fracture-matrix interface, ft
ξ_D	=	normal coordinate to fracture-matrix interface, dimensionless
σ_h^2	=	variance of the matrix block size distribution, ft^2
ϕ_f	=	fracture porosity, dimensionless
ϕ_m	=	matrix porosity, dimensionless
ω_f	=	fracture storativity ratio, dimensionless
ω_m	=	matrix storativity ratio, dimensionless

SI METRIC CONVERSION FACTORS

bbl	x	1.589873	E-01	=	m^3
cp	x	1.0'	E 0 3	=	pa.s
ft	x	3.048'	E-01	=	m
psi	x	6.894757	E-01	=	kpa
psi^{-1}	x	1.450	E 0 1	=	kpa^{-1}

' Conversion factor is exact.

12 BIBLIOGRAPHY

1. Barenblatt, G.E., Zheltov, I.P., and Kochina,I.N.: 'Basic Concepts in the Theory of Homogeneous Liquids in Fissured Rocks,' J. Appl. Math. Mech. 24, (1960), 1286-1303.

2. Barenblatt, G.E.: 'On Certain Boundary-Value Problems for the Equations of Seepage of a Liquid in Fissured Rocks,' J. Appl. Math. Mech., 27, (1963), 513-518.

3. Warren, J.E. and Root, P.J.: 'Behaviour of Naturally Fractured Reservoirs,' Soc. Pet. Eng. J., (Sept. 1963), 245-55.

4. de Swaan, O.A.: 'Analytical Solutions for Determining Naturally Fractured Reservoir Properties by Well Testing,' Soc. Pet. Eng. J., (June 1976).

5. Kazemi, H.: 'Pressure Transient Analysis of Naturally Fractured Reservoirs with Uniform Fracture Distribution,' Soc. Pet. Eng. J., (Dec. 1969), 451-62.

6. Isaacs, C.M.: 'Geology and Physical Properties of the Monterey Formation, California,' paper SPE 12733 presented at the 1984 California Regional Meeting, Long Beach, April 11-13.

7. McQuillan, H.: 'Small Scale Fracture Density in Asmari Formation of Southwest Iran and its Relation to Bed Thickness and Structural Setting,' AAPG Bulletin, V.57, No. 12, (Dec. 1973), 2367-2385.

8. McQuillan, H: 'Fracture Patterns on Kuh-e Asmari Anticline, Southwest Iran,' AAPG Bulletin, V.58, No. 2, (Feb. 1974), 236-246.

9. Stearns, D.W., and Friedman, M.: 'Reservoirs in Fractured Rock,' AAPG Memoir (1972), 82-106.

10. Braester, C.: 'Influence of Block Size on the Transition Curve for a Drawdown Test in a Naturally Fractured Reservoir,' SPEJ 1984, 498-504.

11. Cinco-Ley, H., Samaniego-V, F., and Kucuk, F.: 'The Pressure Transient Behavior for Naturally Fractured Reservoirs with Multiple Block Size,' paper SPE 14168, presented at the 60th Annual Fall Technical Conference and Exhibition, Las Vegas, NV, Sept. 22–25, 1985.

12. Jalali-Yazdi, Y., and Belani, A.: 'Pressure Transient Modeling of Nonuniformly Fractured Reservoirs,' Proceedings of Advances in Geothermal Reservoir Technology, Lawrence Berkeley Laboratory, June 14-15, 1988.

13. Jalali-Yazdi, Y., and Ershaghi, I.: 'Pressure Transient Analysis of Heterogeneous Naturally Fractured Reservoirs,' paper SPE 16341, presented at the SPE California Regional Meeting, Ventura, California, April 8-10, 1987.

14. Jalali-Yazdi, Y., and Ershaghi, I.: 'A Unified Type Curve Approach for Pressure Transient Analysis of Naturally Fractured Reservoirs,' paper SPE 16778 presented at the 62nd Annual Fall Technical Conference and Exhibition, Dallas, TX, Sept 27-30, 1987.

15. Odeh, A.S.: 'Unsteady State Behaviour of Naturally Fractured Reservoirs,' Soc. Pet. Eng. J. (March 1965) 60-66.

16. Kazemi, H., Seth, M.S., Thomas, G.W.: 'The Interpretation of Interference Tests in Naturally Fractured Reservoirs with Uniform Fracture Distribution,' Soc. Pet. Eng. J. (Dec 1969) 463-72.

17. de Swaan, O.: Analytical Solutions for Determining Naturally Fractured Reservoir Properties by Well Testing,' Soc. Pet. Eng. J. (June 1976).

18. Mavor, M.J., Cinco, H.: 'Transient Pressure Behaviour of Naturally Fractured Reservoirs,' Paper SPE 7977 presented at the 1979 SPE California Regional Meeting, Ventura, April 18-20.

19. Najurieta, H.L.: 'A Theory for Pressure Transient Analysis in Naturally Fractured Reservoirs,' J. Pet. Tech. (July 1980) 1241-50.

20. Bourdet, D. and Gringarten, A.: 'Determination of Fissured Volume and Block Size in Naturally Fractured Reservoirs by Type-Curve

Analysis,' paper SPE 9293 presented at the 1980 SPE Annual Technical Conference and Exhibition, Dallas, Sept. 21-24.

21. Bourdet, D. et al.: 'A New Set of Type Curves Simplifies Well Test Analysis,' World Oil (May 1983).

22. Bourdet, D. et al.: 'Interpreting Well Tests in Fractured Reservoirs,' World Oil (Oct.1983).

23. Streltsova, T.D.: 'Well Pressure Behaviour of a Naturally Fractured Reservoir,' Soc. Pet. Eng. J. (Oct.1983) 769-80.

A SOLUTIONS

Combining equations **(1)** and **(2)** from the text,

$$\frac{1}{r}\frac{\partial}{\partial r}(r\frac{\partial P_f}{\partial r}) = \frac{\phi_f c_f \mu}{k_f}\frac{\partial P_f}{\partial t} + \int_{h_{min}}^{h_{max}} Q(h) f(h) dh. \tag{1}$$

Pseudo-Steady State

Considering the direction of **flow** as that of the normal to the matrix-fracture interface, material balance yields:

$$\frac{\partial^2 P_m}{} = \frac{\phi_m c_m \mu}{k_m}\frac{\partial P_m}{at}. \tag{2}$$

For pseudo-steady state, the pressure gradient is a constant in space, hence:

$$\frac{\partial^2 P_m}{\partial \xi^2} = \frac{\phi_m c_m \mu}{k_m}\frac{\partial P_m}{\partial t} = C(t) \tag{3}$$

Integrating twice with respect to ξ,

$$\frac{\partial P_m}{\partial \xi} = C(t)\xi + A, \tag{4}$$

and,

$$P_m = C(t)\frac{\xi^2}{2} + A\xi + B, \tag{5}$$

where A and B are constants. Applying the boundary conditions in ξ,

$P_{D_m} = P_{D_f}$ at $\xi_D = 0$,

$\frac{\partial P_{D_m}}{\partial \xi_D} = 0$ at $\xi_D = 1$,

$$B = P_f \tag{6}$$

$$A = -hC(t) \tag{7}$$

From Darcy's law at the matrix-fracture interface,

$$Q(h) = \frac{-k_m}{\mu h}\frac{\partial P_m}{\partial \xi}|_{interface} \tag{8}$$

which yields,

$$Q(h) = \phi_m c_m \frac{\partial P_m}{\partial t}. \tag{9}$$

Averaging the expression for P_m from **0** to h, Eqn.(5)

$$\frac{\partial P_m}{\partial t} = \frac{3k_m}{\phi_m c_m \mu h^2}(P_f - P_m). \tag{10}$$

Substituting the dimensionless parameters **as** defined before in the text, the equation for **PSS** flow becomes,

$$\frac{\partial^2 P_{D_f}}{\partial r_D^2} + \frac{1}{r_D}\frac{\partial P_{D_f}}{\partial r_D} = \omega_f \frac{\partial P_{D_f}}{\partial t_D} + \omega_m \int_{\frac{h_{min}}{h_{max}}}^{1} \frac{\partial P_{D_m}}{\partial t_D} f(h_D) dh_D, \tag{11}$$

and in the matrix,

$$\frac{\partial P_{D_m}}{\partial t_D} = \frac{3\lambda}{\omega_m}(P_{D_f} - P_{D_m}). \tag{12}$$

To solve the equations **so** obtained, **(11)** and **(12),** we specify the following initial and boundary conditions:

$$P_{D_f} = P_{D_m} = 0 \qquad\qquad t_D = 0.$$

Boundary conditions in the radial direction:

$\lim_{r_D \to \infty} P_{D_f} = 0,$

$\frac{\partial P_{D_f}}{\partial r_D}|_{r_D=1} = -1,$

$C_D \frac{\partial P_{D_w}}{\partial t_D} - (\frac{\partial P_{D_f}}{\partial r_D})_{r_D=1} = 1,$

$P_{D_w} = [P_{D_f} - S_D(\frac{P_{D_f}}{\partial r_D})]_{r_D=1}.$

Transforming this set of equations to Laplace space, and rearranging,

$$r_D^2 \frac{\partial^2 \overline{P}_{D_f}}{\partial r_D^2} + r_D \frac{\partial \overline{P}_{D_f}}{\partial r_D} - r_D^2 sg(s)\overline{P}_{D_f} = 0, \tag{13}$$

where,

$$g(s) = \omega_f + \omega_m \int_{\frac{k_{min}}{k_{max}}}^{1} \frac{3\lambda}{\omega_m s + 3\lambda} f(h_D) dh_D \tag{14}$$

The solution to this equation is the double porosity solution,

$$\overline{P}_{D_w} = \frac{K_0(x) + S_D x K_1(x)}{s[C_D s(K_0(x) + S_D x K_1(x)) + x K_1(x)]}, \tag{15}$$

Unsteady State

A similar procedure can be followed for the unsteady state case, using the matrix flow equation,

$$Q(h) = \frac{-k_m}{\mu h}\frac{\partial P_m}{\partial \xi}|_{interface} \tag{16}$$

and the material balance equation

$$\frac{\partial^2 P_m}{\partial \xi^2} = \frac{\phi_m c_m \mu}{k_m}\frac{\partial P_m}{\partial t}. \tag{17}$$

The initial and boundary conditions are exactly the same as the PSS case . Substituting dimensionless parameters, and transforming to Laplace domain,

$$\frac{\partial^2 \overline{P}_{D_f}}{\partial r_D^2} + \frac{1}{r_D}\frac{\partial \overline{P}_{D_f}}{\partial r_D} = \omega_f s\overline{P}_{D_f} - \int_{\frac{h_{min}}{h_{max}}}^{1} \lambda \frac{\partial \overline{P}_{D_m}}{\partial \xi_D}|_{\xi_D=0} f(h_D)dh_D \tag{18}$$

and,

$$\frac{\partial^2 \overline{P}_{D_m}}{\partial \xi_D^2} = \frac{\omega_m s}{\lambda}\overline{P}_{D_m} \tag{19}$$

Solving equation(19) with the boundary conditions in ξ_D and substituting in eqn(18), we get a form similar to PSS

$$r_D^2\frac{\partial^2 \overline{P}_{D_f}}{\partial r_D^2} + r_D\frac{\partial \overline{P}_{D_f}}{\partial r_D} - r_D^2 sg(s)\overline{P}_{D_f} = 0, \tag{20}$$

where,

$$g(s) = \omega_f + \int_{\frac{h_{min}}{h_{max}}}^{1} \sqrt{\frac{\omega_m \lambda}{s}} tanh\left(\sqrt{\frac{\omega_m s}{\lambda}}\right) f(h_D dh_D \tag{21}$$

The solution is the same as eqn(15) with a different g(s).

B SOFTWARE PROGRAMS

```
C       Program for Pressure response to Uniform Distributions
C     program main

      implicit real*8 (a-h,p-z)
      dimension pda(300),dpda(300),d2pda(300),tda(300)
      common m,red, sk,cbar, slmin, slmax, omegm, ssn, fs, sfs
      open(unit=3,file='datp')
      rewind(unit=3)
              n=10
              m=l
C     slmax =  1.0e-6
C     omegm  =  0.95
C     slmin = 0.8e-6
      print *,'lambda(max) = '
      read *,slmax
      print *, 'lambda(min) = '
      read *,slmin
      print *,'omega = '
      read *,omegm
      print *,'cbar= '
      read *, cbar
      ssn    =  0.0
      sk     =  -2.3
      td=0.1
      do 10 i=1,250
        call pwd(td, n, pd, dpd, d2pd)
        tda(i) = td
        pda(i) = pd
        dpda(i) = dpd*td
        d2pda(i) = d2pd*td*td + dpd*td
        td=td*1.1
 10   continue
      write(3,*)250
      do 20 i=1,250
        write(3,50)tda(i),pda(i)
20    continue
      write(3,*)250
      do 30 i=1,250
        write(3,50)tda(i),dpda(i)
30    continue
C     write(3,*)250
C     do 40 i=1,250
C       d2pda(i) = (dpda(i+1)-dpda(i))/(tda(i+1)-tda(i))*(tda(i+1)+tda(i))
C       write(3,50)tda(i),d2pda(i)
c40   continue
50    format(2f20.4)
70            stop
              end

C               THE STEHFEST ALGORITHM
```

```
C              ******************************
C
      SUBROUTINE PWD(TD,N,PD,dpd,d2pd)
C          THIS FUNTION COMPUTES NUMERICALLY THE LAPLACE TRNSFORM
C          INVERSE OF F(S).

      IMPLICIT REAL*8 (A-H,O-Z)
      DIMENSION G(50),V(50),H(25)
      common m,red,sk,cbar,slmin,slmax,omegm,ssn,fs,sfs
C
C          NOW IF THE ARRAY V(I) WAS COMPUTED BEFORE THE PROGRAM
C          GOES DIRECTLY TO THE END OF THE SUBRUTINE TO CALCULATE
C          F(S).
      IF (N.EQ.M) GO TO 17
      M=N
      DLOGTW-0.6931471805599
      NH=N/2
C
C          THE FACTORIALS OF 1 TO N ARE CALCULATED INTO ARRAY G.
      G(1)=1
      DO 1 I=2,N
         G(I)=G(I-1)*I
1     CONTINUE
C
C          TERMS WITH K ONLY ARE CALCULATED INTO ARRAY H.
      H(1)=2./G(NH-1)
      DO 6 I=2,NH
         FI-I
         IF(I-NH) 4,5,6
4        H(I)=FI**NH*G(2*I)/(G(NH-I)*G(I)*G(I-1))
         GO TO 6
5        H(I)=FI**NH*G(2*I)/(G(I)*G(I-1))
6     CONTINUE
C
C          THE TERMS (-1)**NH+1 ARE CALCULATED.
C          FIRST THE TERM FOR I=1
      SN=2*(NH-NH/2*2)-1
C
C          THE REST OF THE SN'S  ARECALCULATED IN THE MAIN RUTINE.
C
C
C          THE ARRAY V(I) IS CALCULATED.
      DO 7 I=1,N
C
C            FIRST SET V(I)=0
         V(I)=0.
C
C            THE LIMITS FOR K ARE ESTABLISHED.
C            THE LOWER LIMIT IS K1=INTEG((I+1/2))
         K1=(I+1)/2
C
C            THE UPPER LIMIT IS K2=MIN(I,N/2)
         K2=I
         IF (K2-NH) 8,8,9
9        K2=NH
C
C            THE SUMMATION TERM IN V(I) IS CALCULATED.
8        DO 10 K=K1,K2
            IF (2*K-I) 12,13,12
12          IF (I-K) 11,14,11
11          V(I)=V(I)+H(K)/(G(I-K)*G(2*K-I))
            GO TO 10
13          V(I)=V(I)+H(K)/G(I-K)
            GO TO 10
14          V(I)=V(I)+H(K)/G(2*K-I)
10       CONTINUE
```

```
C
C           THE V(I) ARRAY IS FINALLY CALCULATED BY WEIGHTING
C           ACCORDING TO SN.
            V(I)=SN*V(I)
C
C           THE TERM SN CHANGES ITS SIGN EACH ITERATION.
            SN=-SN
7       CONTINUE
C
C           THE NUMERICAL APPROXIMATION IS CALCULATED.
17      A=DLOGTW/TD
        PD-0
        dpd = 0.
        d2pd = 0.
        DO 15 I=1,N
           ARG=A*I
           PD=PD+V(I)*plap(ARG,sk,cbar,omegm,ssn,slmax,slmin)
           dpd=dpd+v(i)*plapd(arg,sk,cbar,omegm,ssn,slmax,slmin)
           d2pd=d2pd+v(i)*plapd2(arg,sk,cbar,omegm,ssn,slmax,slmin)
15      CONTINUE
        PD=PD*A
        dpd=dpd*a
        d2pd=d2pd*a
18      RETURN
        END

        function plap(s,sk,cbar,omegm,ssn,slmax,slmin)

        implicit double precision(a-h,o-z)
        double precision k0,k1
        argmin = dsqrt(3*slmin/omegm/s)
        argmax = dsqrt(3*slmax/omegm/s)
        hratio = dsqrt(slmin/slmax)
c       fs = (1.0-omegm)-(omegm*argmin*(datan(argmin)-datan(argmax)))/(1-hratio)
        arg1 = omegm*argmin*(datan(argmin)-datan(argmax))/(1-hratio)
        fs = 1.0 - omegm - argl
        sfs=s*fs
        x-dsqrt(sfs)
        y=dsqrt(sfs)
        k1 = dbsk1(x)
        k0 = dbsk0(x)
        plap=((k0 +(sk*x*k1)))/(s*((x*k1)+(cbar*s*(k0+sk*x*k1))))
        return
        end

        function plapd(s,sk,cbar,omegm,ssn,slmax,slmin)

        implicit double precision(a-h,o-z)
        double precision k0,k1
        argmin = dsqrt(3*slmin/omegm/s)
        argmax = dsqrt(3*slmax/omegm/s)
        hratio = dsqrt(slmin/slmax)
c       fs = (1.0-omegm)-(omegm*argmin*(datan(argmin)-datan(argmax)))/(1-hratio)
        argl = omegm*argmin*(datan(argmin)-datan(argmax))/(1-hratio)
        fs = 1.0 - omegm - argl
        sfs=s*fs
        x=dsqrt(sfs)
        y=dsqrt(sfs)
        k1 = dbsk1(x)
        k0 = dbsk0(x)
        plapd=((k0 +(sk*x*k1)))/(1*((x*k1)+(cbar*s*(k0+sk*x*k1))))
        return
        end

        function plapd2(s,sk,cbar,omegm,ssn,slmax,slmin)
```

```
      implicit double precision (a-h,o-z)
      double precision k0,k1
      argmin = dsqrt(3*slmin/omegm/s)
      argmax = dsqrt(3*slmax/omegm/s)
      hratio = dsqrt(slmin/slmax)
c     fs = (1.0-omegm)-(omegm*argmin*(datan(argmin)-datan(argmax)))/(1-hratio)
      argl = omegm*argmin*(datan(argmin)-datan(argmax))/(1-hratio)
      fs  =  1.0 - omegm - argl
      sfs=s*fs
      x=dsqrt(sfs)
      y=dsqrt(sfs)
      k1 = dbsk1(x)
      k0 = dbsk0(x)
      plapd2=s*((k0 +(sk*x*k1)))/(1*((x*k1)+(cbar*s*(k0+sk*x*k1))))
      return
      end
```

```
      FI=I
      IF(I-NH) 4,5,6
4     H(I)=FI**NH*G(2*I)/(G(NH-I)*G(I)*G(I-1))
      GO TO 6
5     H(I)=FI**NH*G(2*I)/(G(I)*G(I-1))
6   CONTINUE
C
C       THE TERMS (-1)**NH+1 ARE CALCULATED.
C       FIRST THE TERM FOR 1=1
    SN=2*(NH-NH/2*2)-1
C
C       THE REST OF THE SN'S  ARECALCULATED IN THE MAIN RUTINE.
C
C
C       THE ARRAY V(I)  IS CALCULATED.
    DO 7 I=1,N
C
C       FIRST SET V(I)=0
      V(I)=0.
C
C       THE LIMITS FOR K ARE ESTABLISHED.
C       THE LOWER LIMIT IS K1=INTEG((I+1/2))
      K1=(I+1)/2
C
C       THE UPPER LIMIT IS K2=MIN(I,N/2)
      K2-I
      IF (K2-NH) 8,8,9
9     K2=NH
C
C       THE SUMMATION TERM IN V(I)  IS CALCULATED.
8     DO 10 K=K1,K2
        IF (2*K-I) 12,13,12
12      IF (I-K) 11,14,11
11      V(I)=V(I)+H(K)/(G(I-K)*G(2*K-I))
        GO TO 10
13      V(I)=V(I)+H(K)/G(I-K)
        GO TO 10
14      V(I)=V(I)+H(K)/G(2*K-I)
10    CONTINUE
C
C       THE V(I) ARRAY IS FINALLY CALCULATED BY WEIGHTING
C       ACCORDING TO SN.
      V(I)=SN*V(I)
C
C       THE TERM SN CHANGES ITS SIGN EACH ITERATION.
      SN=-SN
7   CONTINUE
C
C       THE NUMERICAL APPROXIMATION IS CALCULATED.
17  A=DLOGTW/TD
    PD=0
    dpd = 0.
    DO 15 I=1,N
      ARG=A*I
      PD=PD+V(I)*plap(ARG,sk,cbar,omegm,ssn,sl1,sl2,sl3,sl4)
      dpd=dpd+v(i)*plapd(arg,sk,cbar,omegm,ssn,sl1,sl2,sl3,sl4)
15  CONTINUE
    PD=PD*A
    dpd=dpd*a
18  RETURN
    END

    function plap(s,sk,cbar,omegm,ssn,sl1,sl2,sl3,sl4)

    implicit real*8 (a-h,o-z)
    real*8 k0,k1
```

```
      double precision mmbsk0,mmbsk1
      integer iopt,ier
      iopt=1
      argl = dsqrt(3*sl1/omegm/s)
      arg2 = dsqrt(3*sl2/omegm/s)
      arg3 = dsqrt(3*sl3/omegm/s)
      arg4 = dsqrt(3*sl4/omegm/s)
      hlrat = dsqrt(sl1/sl4)
      h2rat = dsqrt(sl1/sl3)
      h3rat = dsqrt(sl1/sl2)
      denom = 1-h3rat+h2rat-h1rat
c     fs = (1.0-omegm)-(omegm*arg1*(datan(arg1)-datan(arg2)))/denom
      arg12 = omegm*arg1*(datan(arg1)-datan(arg2))/denom
      arg34 = omegm*arg1*(datan(arg3)-datan(arg4))/denom
      fs = 1.0 - omegm - arg12 - arg34
      sfs=s*fs
      x-dsqrt(sfs)
      y=dsqrt(sfs)
      k1 = mmbsk1(iopt,x,ier)
      k0 = mmbsk0(iopt,x,ier)
      plap-((k0 +(sk*x*k1)))/(s*((x*k1)+(cbar*s*(k0+sk*x*k1))))
      return
      end

      function plapd(s,sk,cbar,omegm,ssn,sl1,sl2,sl3,sl4)

      implicit real*8(a-h,o-z)
      real*8 k0,k1
      double precision mmbsk0,mmbsk1
      integer iopt,ier
      iopt=1
      argl = dsqrt(3*sl1/omegm/s)
      arg2 = dsqrt(3*sl2/omegm/s)
      arg3 = dsqrt(3*sl3/omegm/s)
      arg4 = dsqrt(3*sl4/omegm/s)
      hlrat = dsqrt(sl1/sl4)
      h2rat = dsqrt(sl1/sl3)
      h3rat = dsqrt(sl1/sl2)
      denom = 1-h3rat+h2rat-h1rat
c     fs = (1.0-omegm)-(omegm*arg1*(datan(arg1)-datan(arg2)))/denom
      arg12 = omegm*arg1*(datan(argl)-datan(arg2))/denom
      arg34 = omegm*arg1*(datan(arg3)-datan(arg4))/denom
      fs = 1.0 - omegm - arg12 - arg34
      sfs=s*fs
      x=dsqrt(sfs)
      y=dsqrt(sfs)
      k1 = mmbskl(iopt,x,ier)
      k0 = mmbsk0(iopt,x,ier)
      plapd=((k0 +(sk*x*k1)))/(1*((x*k1)+(cbar*s*(k0+sk*x*k1))))
      return
      end
```

```
C       Program for Pressure response to Uniform Distribution (Unsteady
C       State)
C     program main

      implicit real*8 (a-h,p-z)
      dimension pda(300),dpda(300),d2pda(300),tda(300)
      common m,red,sk,cbar,slmin,slmax,omegm,ssn,fs,sfs,ans
      open(unit=3,file='datp')
      rewind(unit=3)
            n=10
            m=1
C     slmax =  1.0e-6
C     omegm  =  0.95
C     slmin = 0.8e-6
      print *,'lambda(max) = '
      read *,slmax
      print *,'lambda (min) = '
      read *,slmin
      print *,'omega = '
      read *,omegm
      ssn    =  0.0
      sk     =  0.0
      cbar   =  0.0
      td=0.1
      do 10 i=1,250
        call pwd(td,n,pd,dpd)
        tda(i) = td
        pda(i) = pd
        dpda(i) = dpd*td
C       d2pda(i) = d2pd*td*td + dpd*td
        td=td*1.1
 10   continue
      write(3,*)250
      do 20 i=1,250
        write(3,50)tda(i),pda(i)
20    continue
      write(3,*)250
      do 30 i=1,250
        write(3,50)tda(i),dpda(i)
30    continue
C     write(3,*)250
C     do 40 i=1,250
C       d2pda(i) = (dpda(i+1)-dpda(i))/(tda(i+1)-tda(i))*(tda(i+1)+tda(i))
C       write(3,50)tda(i),d2pda(i)
c40   continue
50    format(2f20.4)
70          stop
            end

C              THE STEHFEST ALGORITHM
C            ****************************
C
      SUBROUTINE PWD(TD, N, PD, dpd)
C          THIS FUNTION COMPUTES NUMERICALLY THE LAPLACE TRNSFORM
C          INVERSE OF F(S).

      IMPLICIT  REAL*8 (A-H,O-Z)
      DIMENSION G(50),V(50),H(25)
      external f
      common m,red,sk,cbar,slmin,slmax,omegm,ssn,fs,sfs,ans
C
C          NOW IF THE ARRAY V(I) WAS COMPUTED BEFORE THE PROGRAM
C          GOES DIRECTLY TO THE END OF THE SUBRUTINE TO CALCULATE
C          F(S).
      IF (N.EQ.M) GO TO 17
      M=N
```

```
      DLOGTW=0.6931471805599
      NH=N/2
C
C           THE FACTORIALS OF 1 TO N ARE CALCULATED INTO ARRAY G.
      G(1)=1
      DO 1 I=2,N
         G(I)=G(I-1)*I
1     CONTINUE
C
C           TERMS WITH K ONLY ARE CALCULATED INTO ARRAY H.
      H(1)=2./G(NH-1)
      DO 6 I=2,NH
         FI=I
         IF(I-NH) 4,5,6
4        H(I)=FI**NH*G(2*I)/(G(NH-I)*G(I)*G(I-1))
         GO TO 6
5        H(I)=FI**NH*G(2*I)/(G(I)*G(I-1))
6     CONTINUE
C
C           THE TERMS (-1)**NH+1 ARE CALCULATED.
C           FIRST THE TERM FOR 1=1
      SN=2*(NH-NH/2*2)-1
C
C           THE REST OF THE SN'S ARECALCULATED IN THE MAIN RUTINE.
C
C
C           THE ARRAY V(I) IS CALCULATED.
      DO 7 I=1,N
C
C           FIRST SET V(I)=0
         V(I)=0.
C
C           THE LIMITS FOR K ARE ESTABLISHED.
C           THE LOWER LIMIT IS K1=INTEG((I+1/2))
         K1=(I+1)/2
C
C           THE UPPER LIMIT IS K2=MIN(I,N/2)
         K2=I
         IF (K2-NH) 8,8,9
9        K2=NH
C
C           THE SUMMATION TERM IN V(I) IS CALCULATED.
8        DO 10 K=K1,K2
            IF (2*K-I) 12,13,12
12          IF (I-K) 11,14,11
11          V(I)=V(I)+H(K)/(G(I-K)*G(2*K-I))
            GO TO 10
13          V(I)=V(I)+H(K)/G(I-K)
            GO TO 10
14          V(I)=V(I)+H(K)/G(2*K-I)
10       CONTINUE
C
C           THE V(I) ARRAY IS FINALLY CALCULATED BY WEIGHTING
C           ACCORDING TO SN.
         V(I)=SN*V(I)
C
C           THE TERM SN CHANGES ITS SIGN EACH ITERATION.
         SN=-SN
7     CONTINUE
C
C           THE NUMERICAL APPROXIMATION IS CALCULATED.
17    A=DLOGTW/TD
      PD=0
      dpd = 0.
c      d2pd = 0.
      DO 15 I=1,N
```

```
      ARG=A*I
      dlim = dsqrt(omegm*arg/slmax)
      ulim = dsqrt(omegm*arg/slmin)
      call dqdags(f,dlim,ulim,0.0001,0.0001,ans,err)
      PD=PD+V(I)*plap(ARG,sk,cbar,omegm,ssn,slmax,slmin,ans)
      dpd=dpd+v(i)*plapd(arg,sk,cbar,omegm,ssn,slmax,slmin,ans)
c      d2pd=d2pd+v(i)*plapd2(arg,sk,cbar,omegm,ssn,slmax,slmin,ans)
15    CONTINUE
      PD=PD*A
      dpd=dpd*a
c     d2pd=d2pd*a
18    RETURN
      END

      function plap(s,sk,cbar,omegm,ssn,slmax,slmin,ans)

      implicit real*8 (a-h,o-z)
      real*8 k0,k1
      double precision mmbsk0,mmbsk1
      integer iopt,ier
      iopt=1
      hratio = dsqrt(slmin/slmax)
      argl = dsqrt(slmin*omegm/s)*ans/(1-hratio)
      fs  =  1.0 - omegm + argl
      sfs=s*fs
      x=dsqrt(sfs)
      k1 = mmbskl(iopt,x,ier)
      k0 = mmbsk0(iopt,x,ier)
      plap=((k0 +(sk*x*k1)))/(s*((x*k1)+(cbar*s*(k0+sk*x*k1))))
      return
      end

      function plapd(s,sk,cbar,omegm,ssn,slmax,slmin,ans)

      implicit real*8 (a-h,o-z)
      real*8 k0,k1
      double precision mmbsk0,mmbsk1
      integer iopt,ier
      iopt=1
      hratio = dsqrt(slmin/slmax)
      argl = dsqrt(slmin*omegm/s)*ans/(1-hratio)
      fs  =  1.0 - omegm + argl
      sfs=s*fs
      x=dsqrt(sfs)
      y=dsqrt(sfs)
      k1 = mmbskl(iopt,x,ier)
      k0 = mmbsk0(iopt,x,ier)
      plapd=((k0 +(sk*x*k1)))/(1*((x*k1)+(cbar*s*(k0+sk*x*k1))))
      return
      end

c     function plapd2(s,sk,cbar,omegm,ssn,slmax,slmin,ans)
c
c     implicit real*8(a-h,o-z)
c     real*8 k0,k1
c     double precision mmbsk0,mmbsk1
c     integer iopt,ier
c     iopt=1
c     hratio = dsqrt(slmin/slmax)
c     argl = dsqrt(slmin*omegm/s)*ans/(1-hratio)
c     fs  =  1.0 - omegm + argl
c     sfs=s*fs
c     x=dsqrt(sfs)
c     k1 = mmbskl(iopt,x,ier)
c     k0 = mmbsk0(iopt,x,ier)
c     plapd2=s*((k0 +(sk*x*k1)))/(1*((x*k1)+(cbar*s*(k0+sk*x*k1))))
```

```
c       return
c       end

        function f(x)
        implicit real*8 (a-h,o-z)
        f=dtanh(x)/x
        return
        end
```

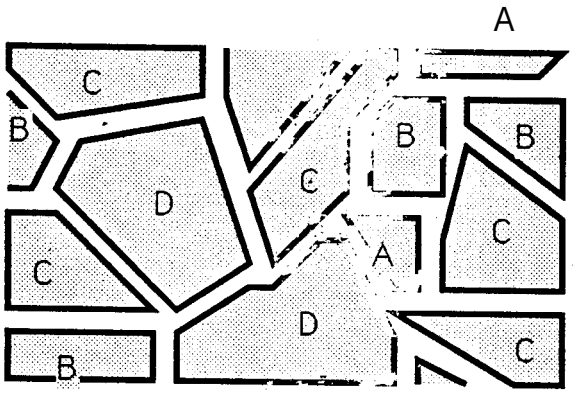

Fig. 1 Non-Uniformly Fractured Reservoir

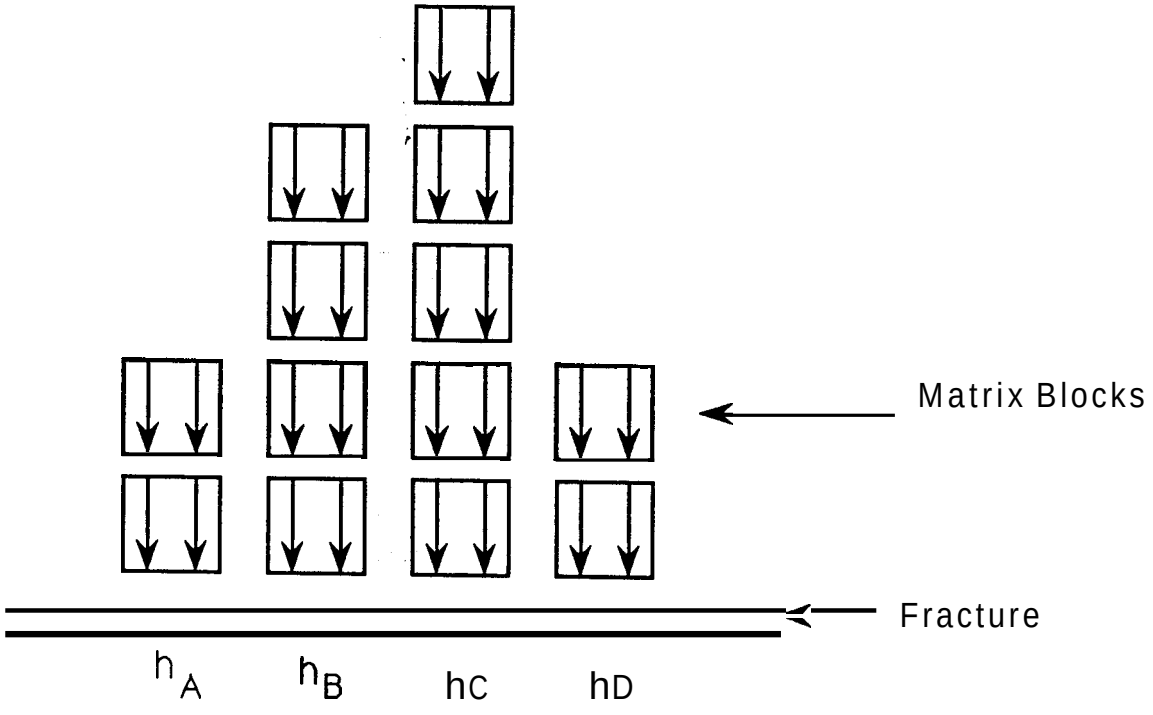

Fig.2 - Matrix Block Size Distribution

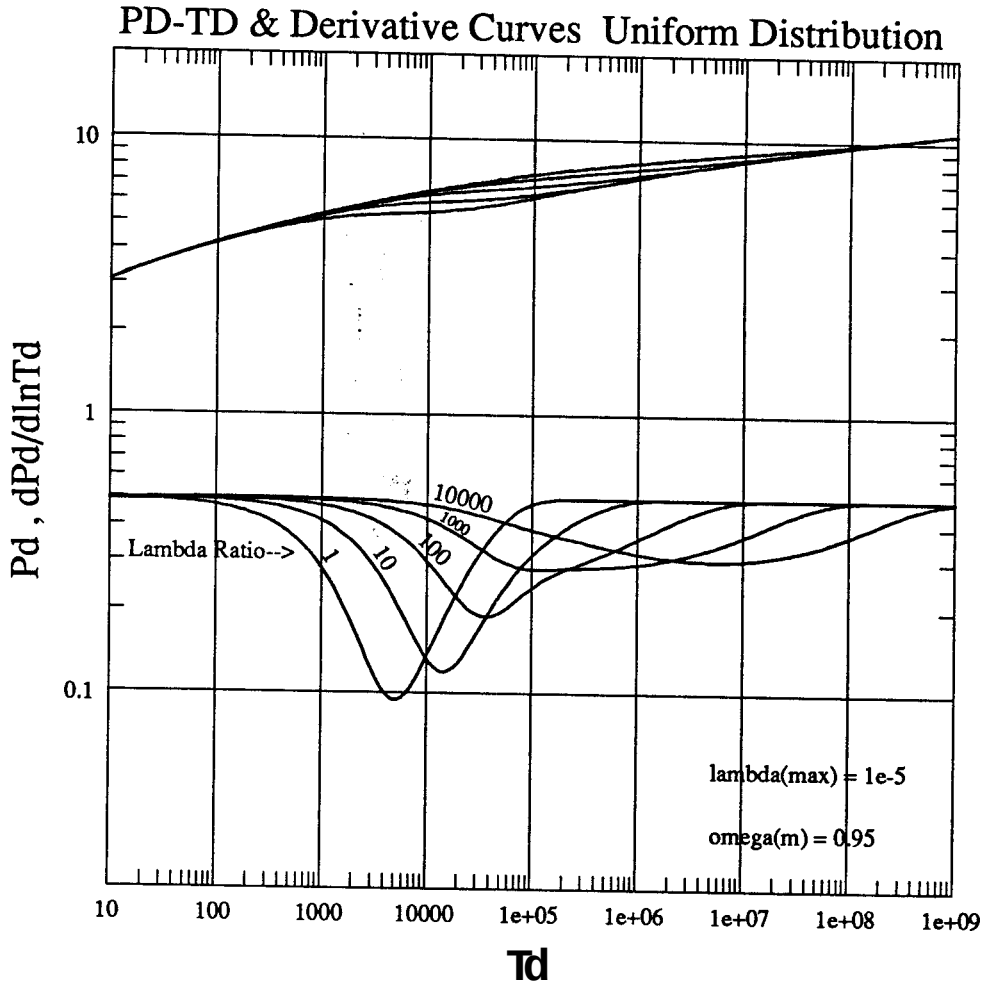

Fig. **3** - Lambda Range le-5 to **le-9**

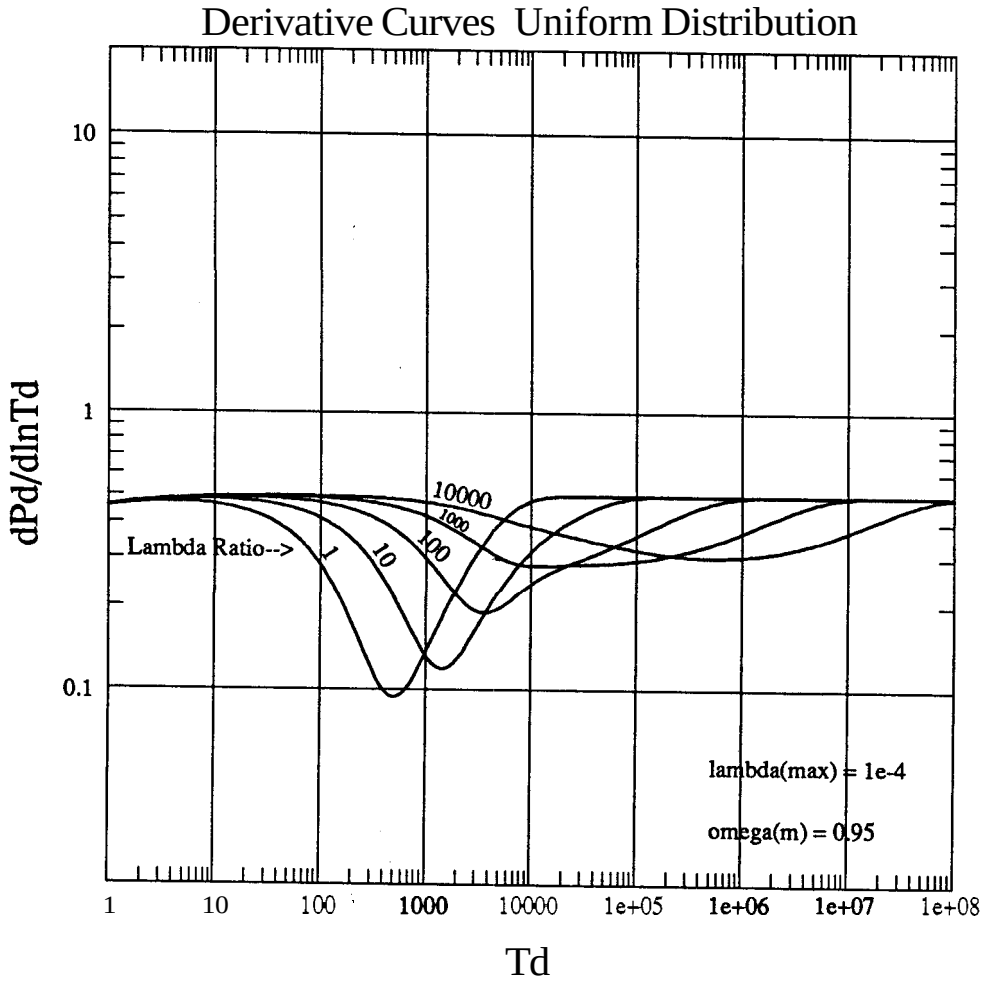

Fig. **4** - Lambda Range le-4 to le-8

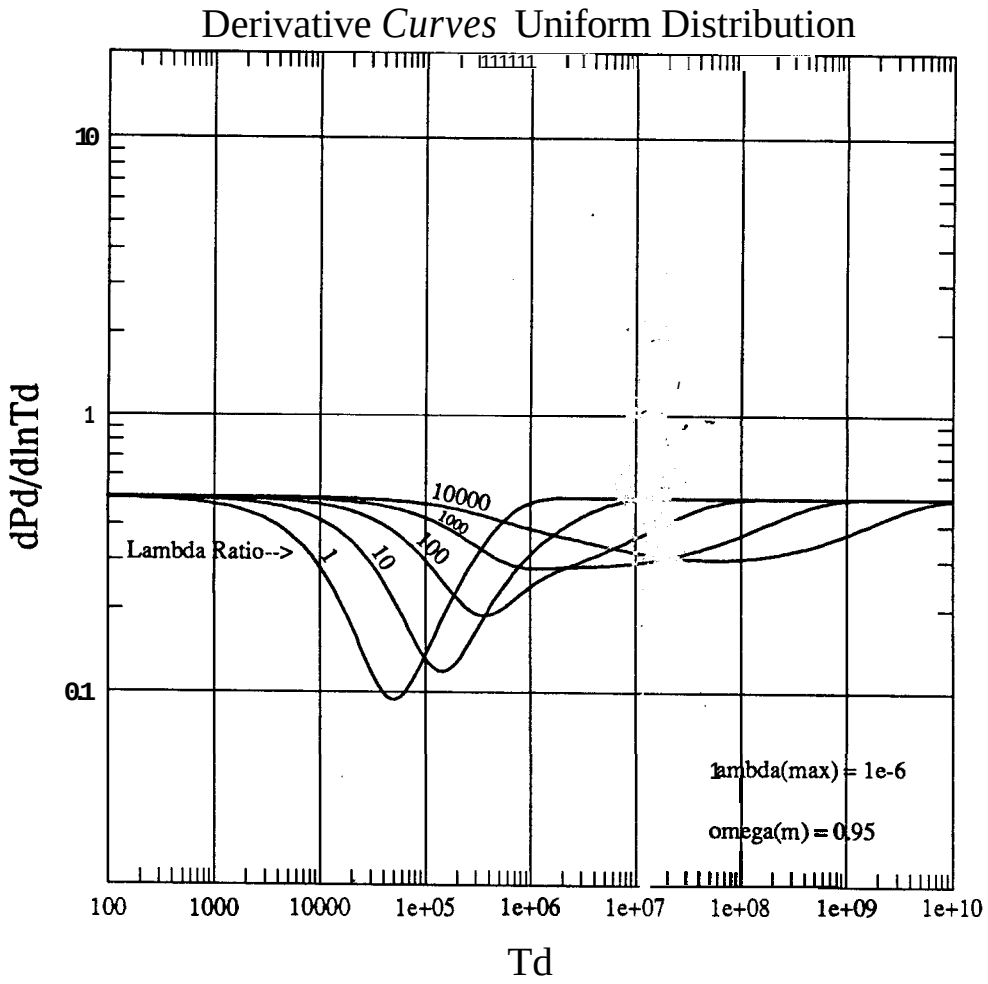

Fig. **5** - Lambda range 1***e-6*** to le-**10**

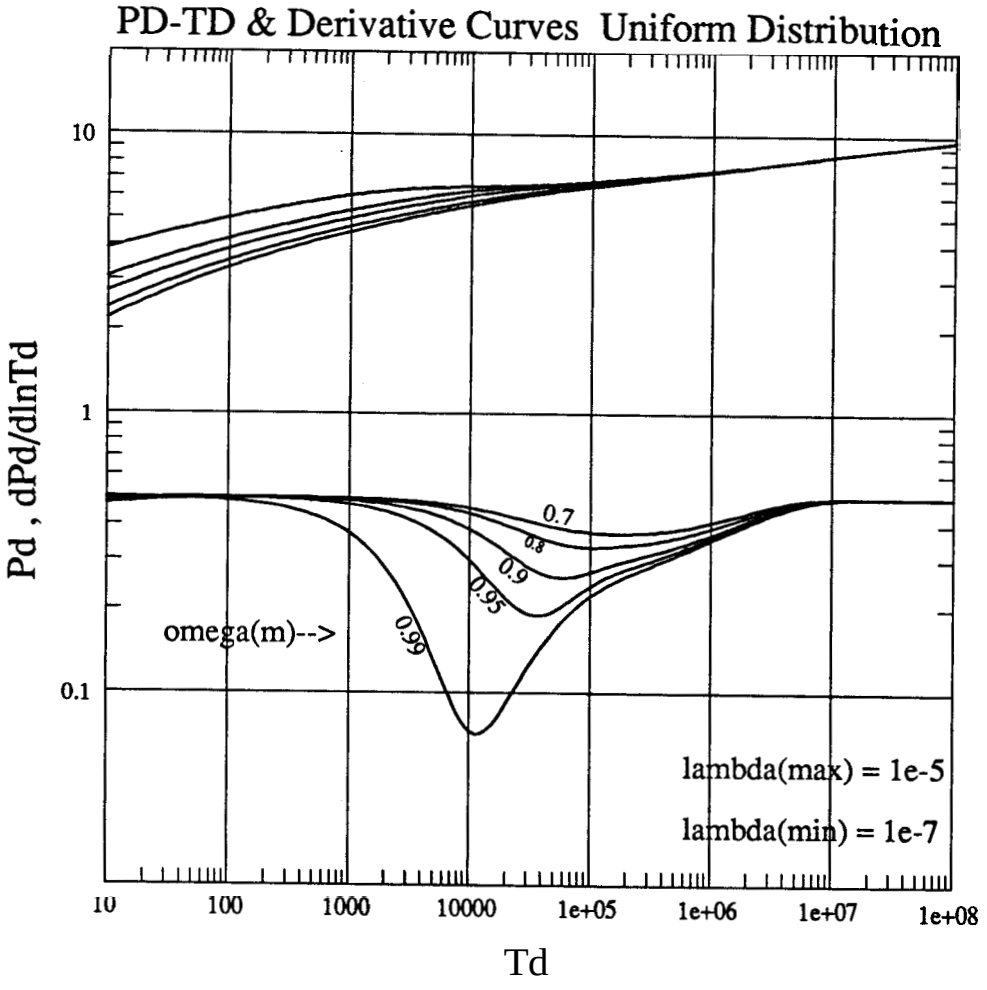
PD-TD & Derivative Curves Uniform Distribution
Pd , dPd/dlnTd
10
1
0.1
0.7
0.8
0.9
0.95
0.99
omega(m)-->
lambda(max) = 1e-5
lambda(min) = 1e-7
10
100
1000
10000
1e+05
1e+06
1e+07
1e+08
Td

Fig. 6

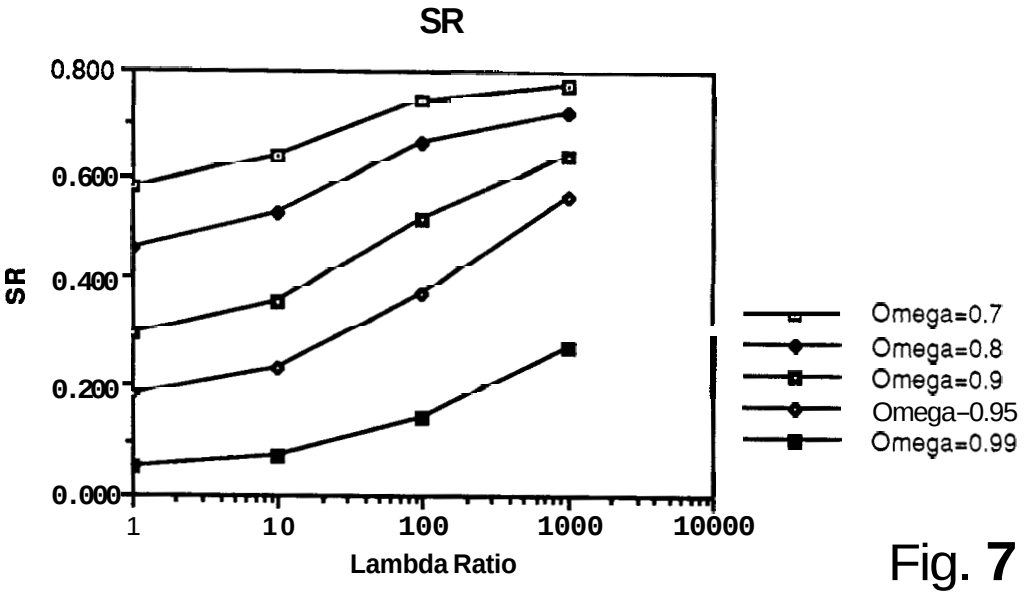
SR
0.800
0.600
0.400
0.200
0.000
SR
1
10
100
1000
10000
Lambda Ratio
Omega=0.7
Omega=0.8
Omega=0.9
Omega–0.95
Omega=0.99

Fig. **7**

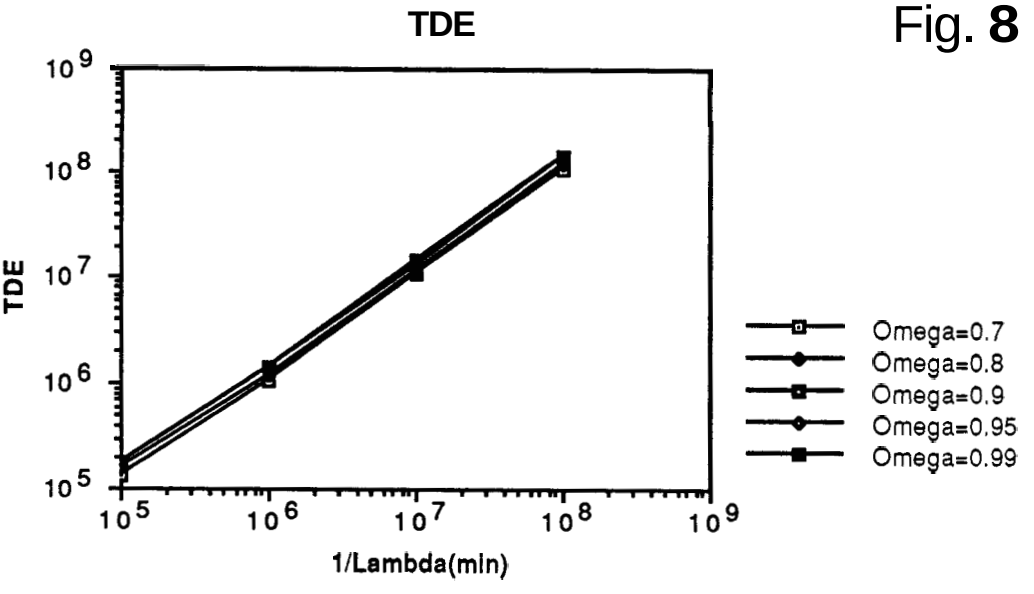
TDE
10^9
10^8
10^7
10^6
10^5
TDE
10^5
10^6
10^7
10^8
10^9
1/Lambda(min)
Omega=0.7
Omega=0.8
Omega=0.9
Omega=0.95
Omega=0.99

Fig. **8**

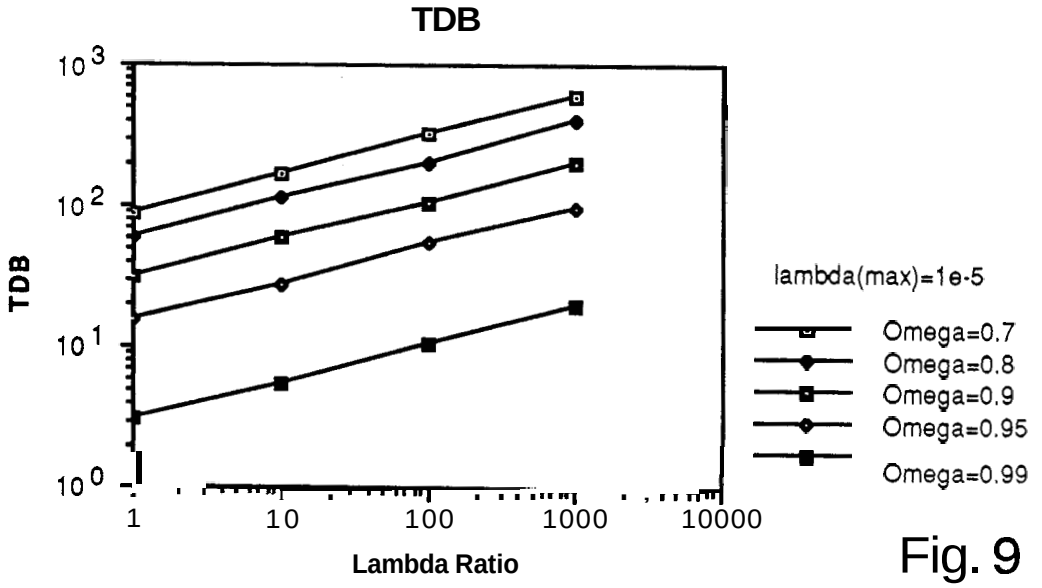
TDB
10^3
10^2
10^1
10^0
TDB
1
10
100
1000
10000
Lambda Ratio
lambda(max)=1e-5
Omega=0.7
Omega=0.8
Omega=0.9
Omega=0.95
Omega=0.99

Fig. 9

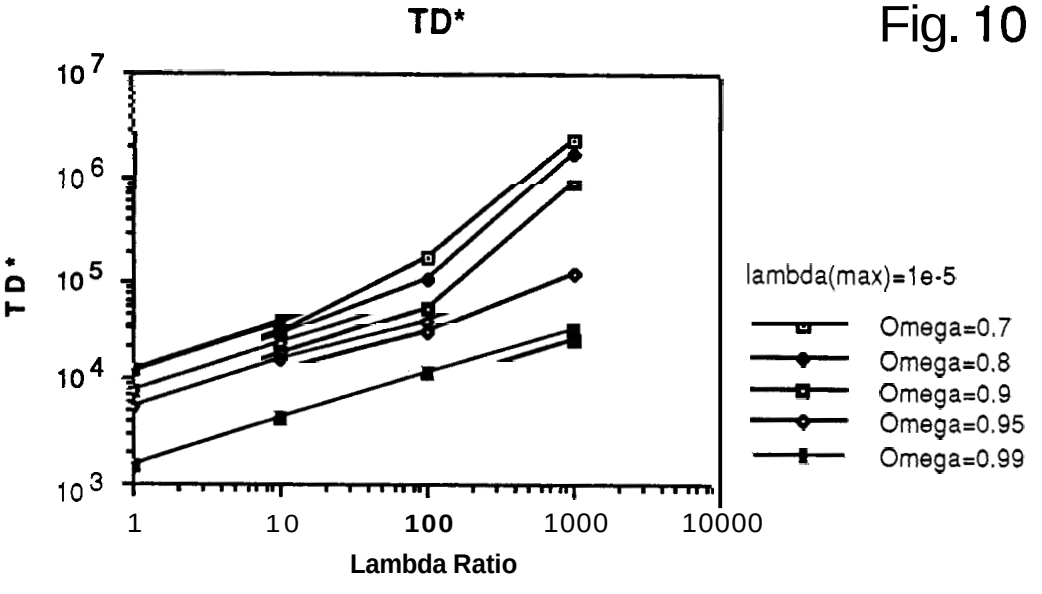
TD*
10^7
10^6
10^5
10^4
10^3
TD*
1
10
100
1000
10000
Lambda Ratio
lambda(max)=1e-5
Omega=0.7
Omega=0.8
Omega=0.9
Omega=0.95
Omega=0.99

Fig. 10

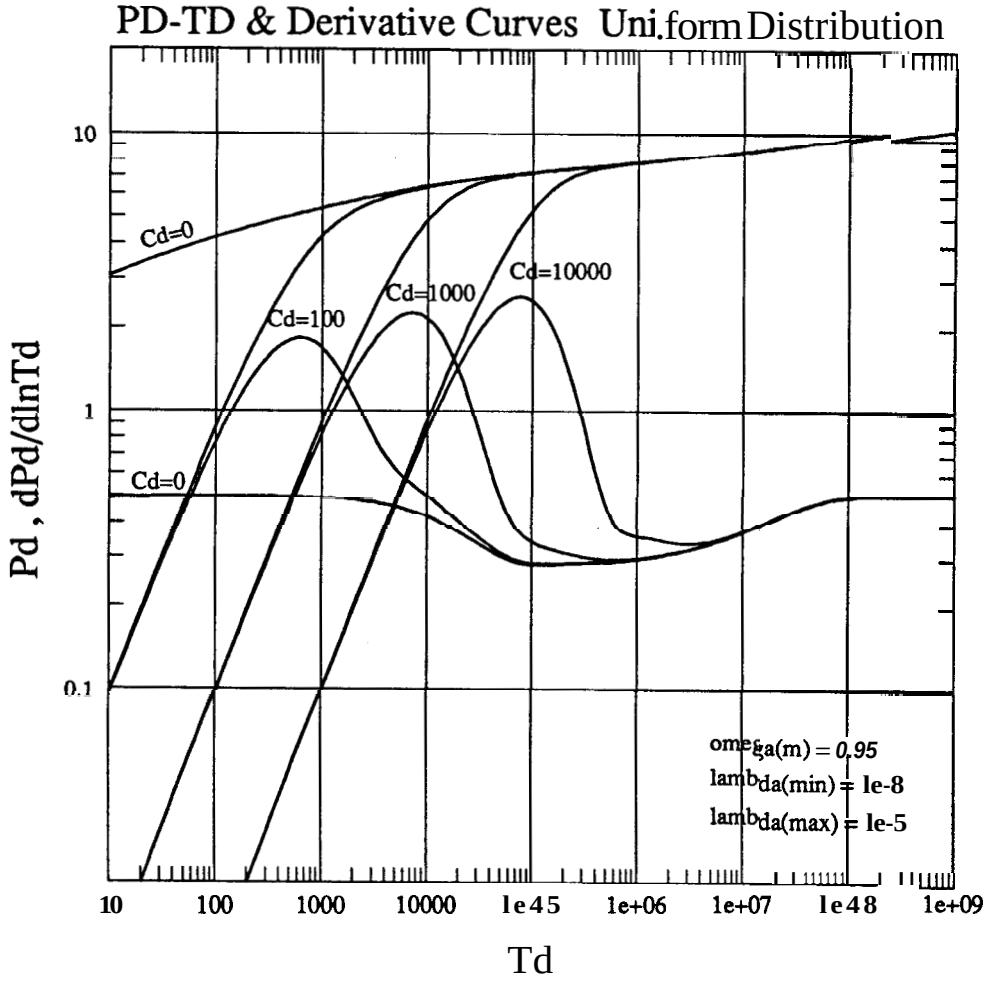
PD-TD & Derivative Curves Uni.form Distribution
Pd , dPd/dlnTd
10
1
0.1
Cd=0
Cd=100
Cd=1000
Cd=10000
Cd=0
omega(m) = 0.95
lambda(min) = le-8
lambda(max) = le-5
10
100
1000
10000
le45
1e+06
1e+07
le48
1e+09
Td

Fig. 11

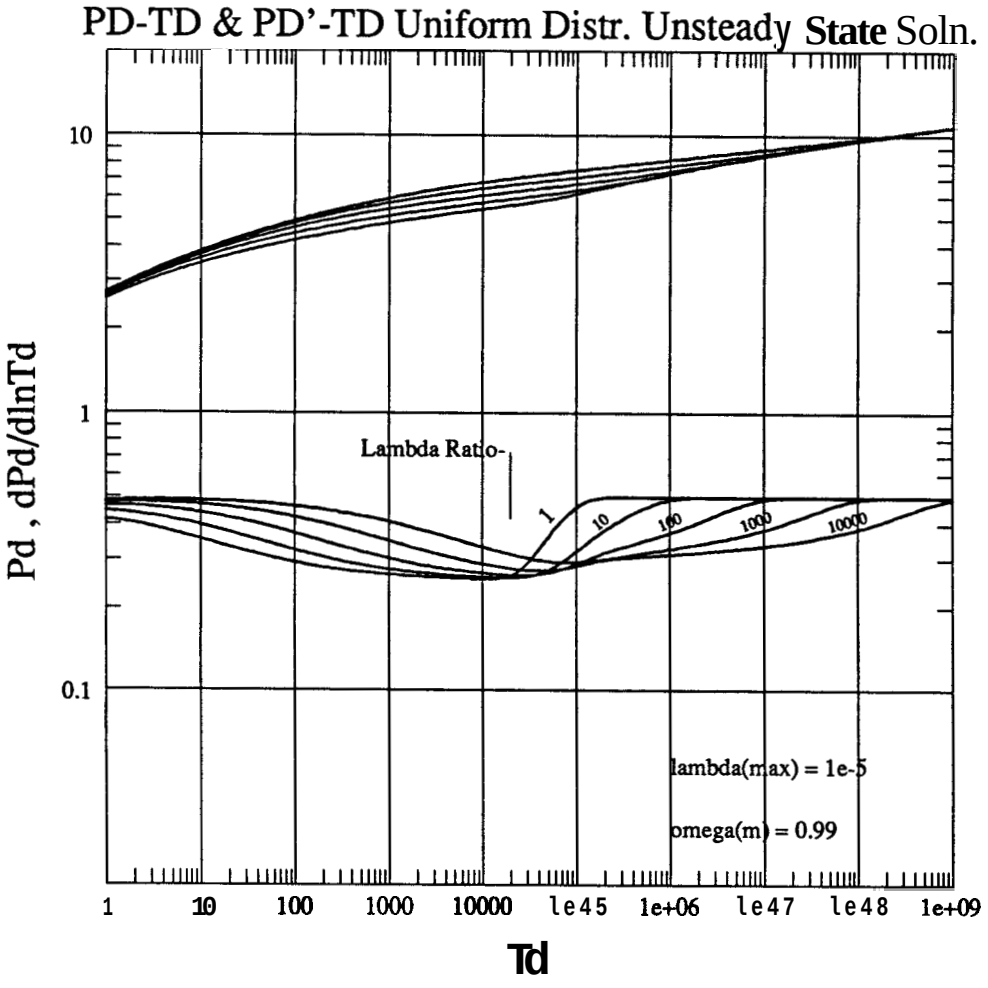
PD-TD & PD'-TD Uniform Distr. Unsteady State Soln.
Pd , dPd/dlnTd
10
1
0.1
Lambda Ratio-
1
10
100
1000
10000
lambda(max) = 1e-5
omega(m) = 0.99
1
10
100
1000
10000
le45
1e+06
le47
le48
1e+09
Td

Fig. 12

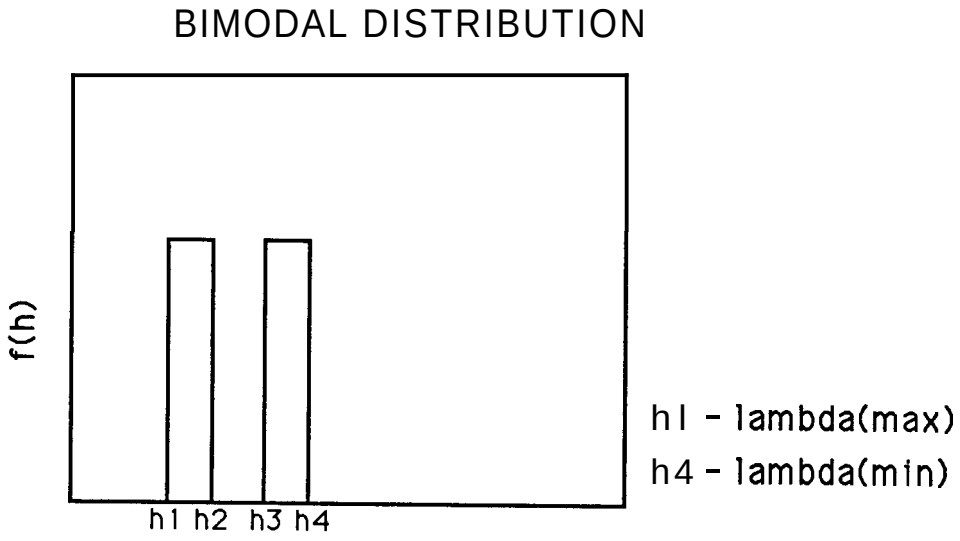
BIMODAL DISTRIBUTION
f(h)
h1 h2 h3 h4
h1 - lambda(max)
h4 - lambda(min)

Fig. 13

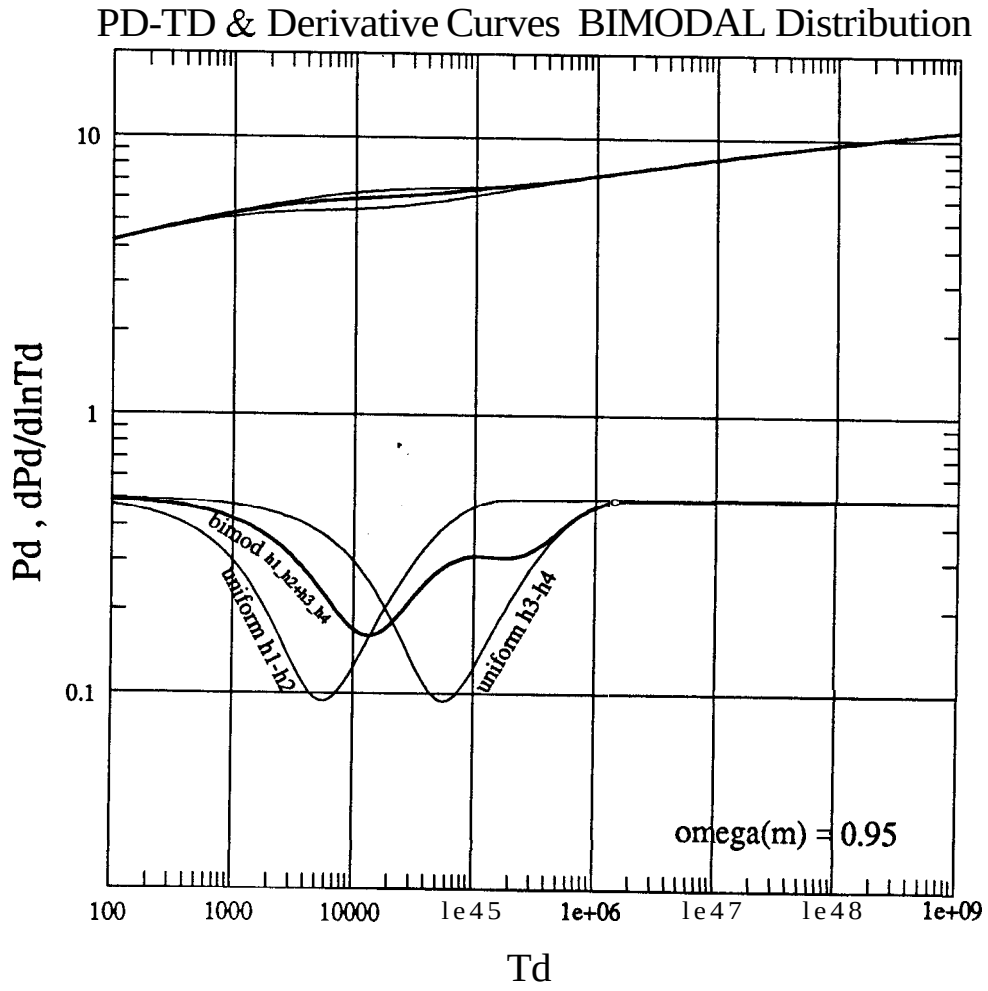
PD-TD & Derivative Curves BIMODAL Distribution
Pd , dPd/dlnTd
10
1
0.1
bimod h1_h2+h3_h4
uniform h1-h2
uniform h3-h4
omega(m) = 0.95
100
1000
10000
1e45
1e+06
1e47
1e48
1e+09
Td

Fig. 14

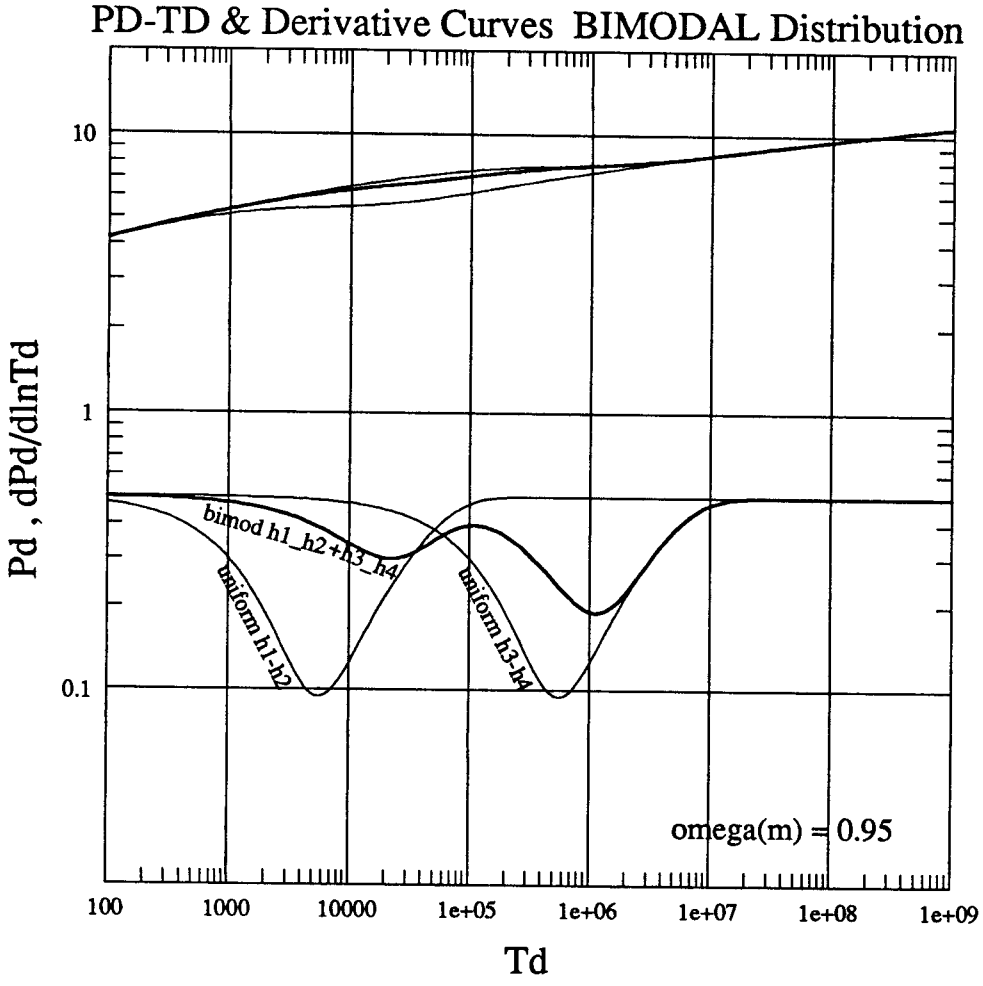
PD-TD & Derivative Curves BIMODAL Distribution
Pd , dPd/dlnTd
10
1
0.1
bimod h1_h2+h3_h4
uniform h1-h2
uniform h3-h4
omega(m) = 0.95
100
1000
10000
1e+05
1e+06
1e+07
1e+08
1e+09
Td

Fig. 15

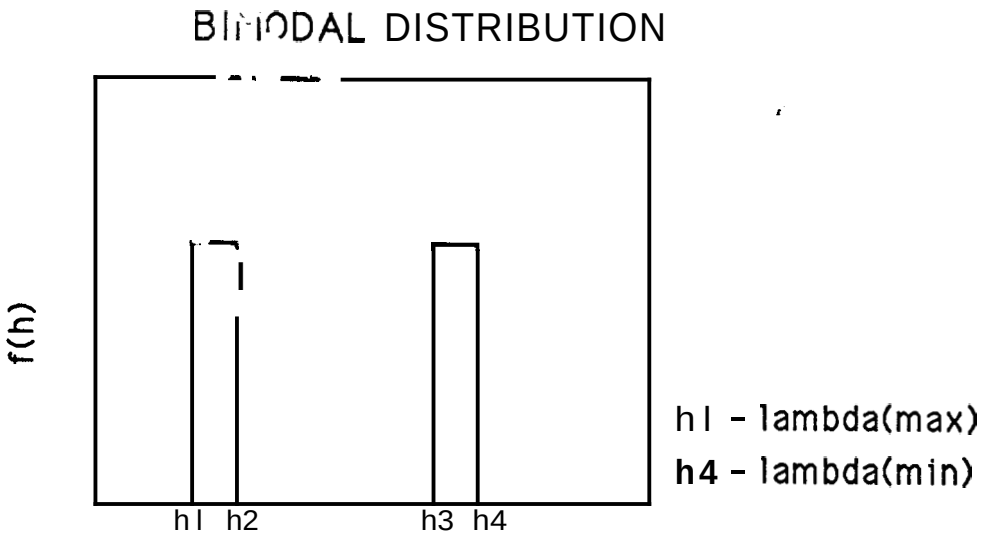
BIMODAL DISTRIBUTION
f(h)
h1 - lambda(max)
h4 - lambda(min)
h1 h2
h3 h4

Fig. 16

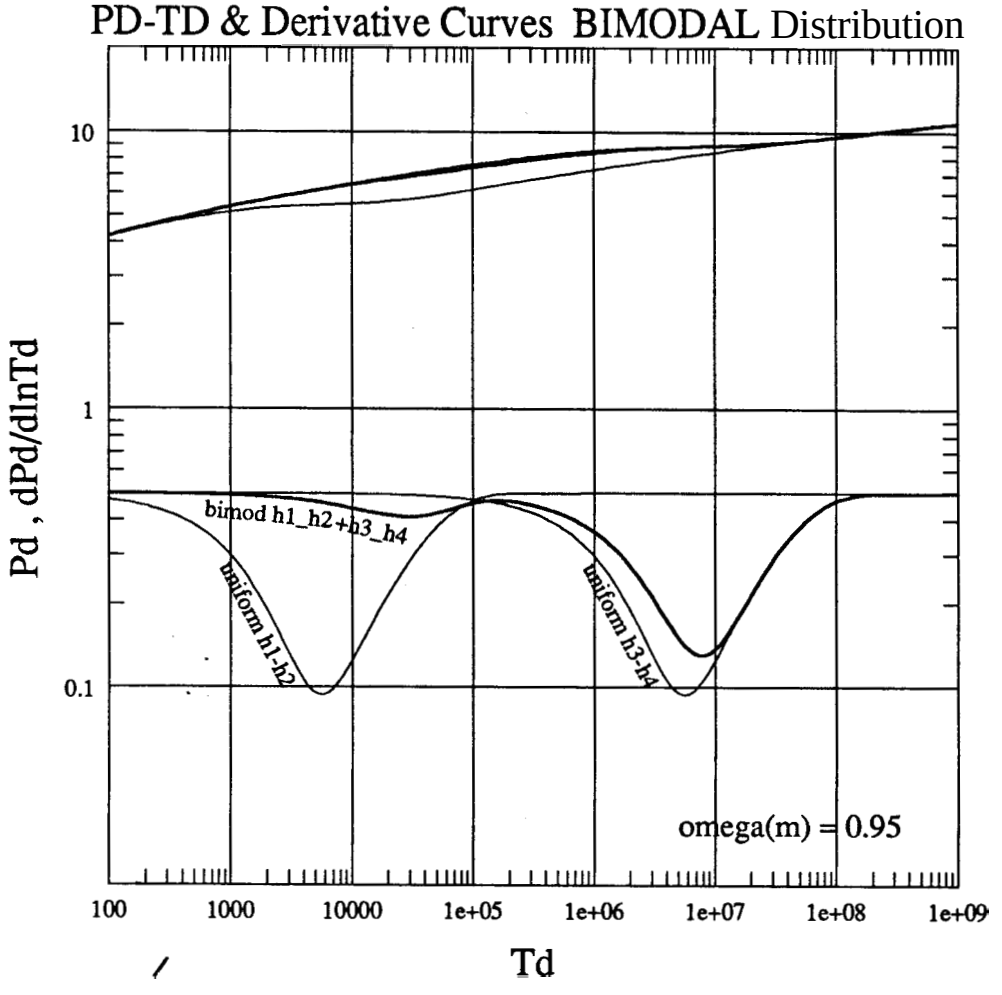
PD-TD & Derivative Curves BIMODAL Distribution
Pd , dPd/dlnTd
10
1
0.1
bimod h1_h2+h3_h4
uniform h1-h2
uniform h3-h4
omega(m) = 0.95
100
1000
10000
1e+05
1e+06
1e+07
1e+08
1e+09
Td

Fig. 17

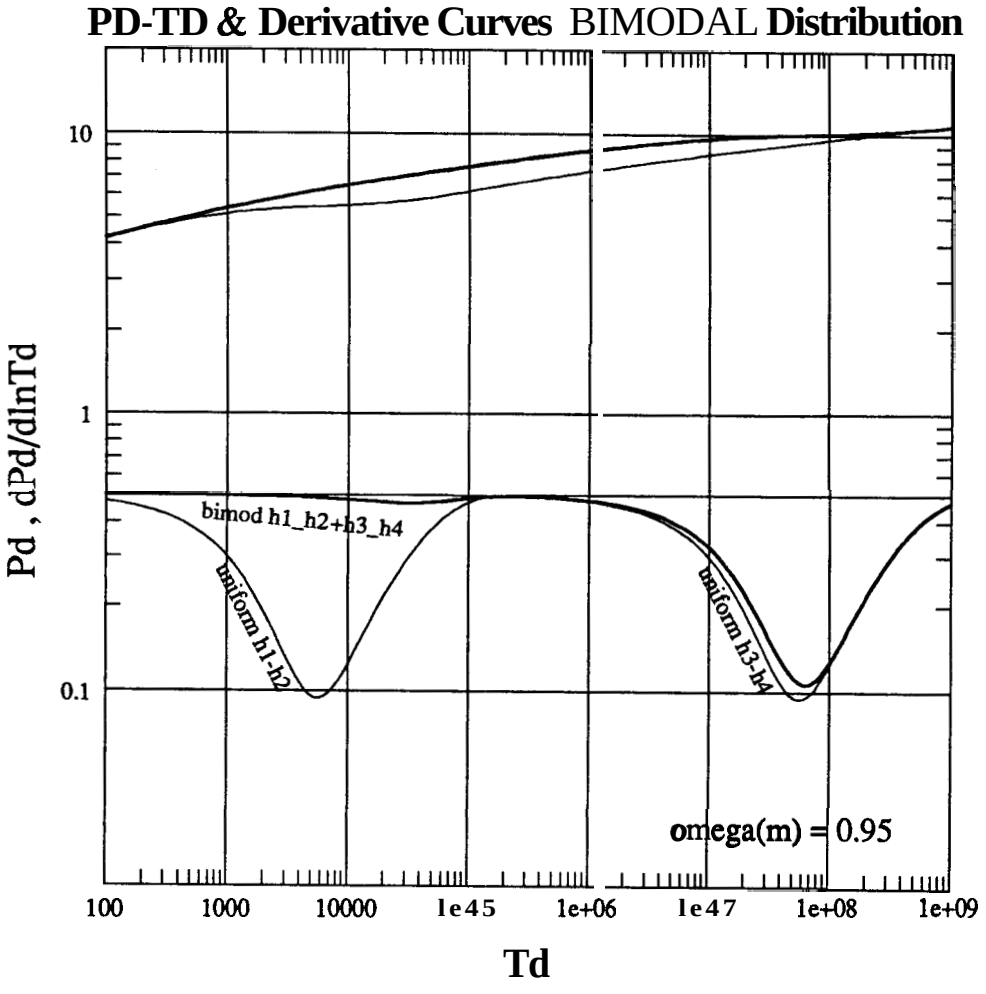
PD-TD & Derivative Curves BIMODAL Distribution
10
1
0.1
Pd , dPd/dlnTd
bimod h1_h2+h3_h4
uniform h1-h2
uniform h3-h4
omega(m) = 0.95
100
1000
10000
1e45
1e+06
1e47
1e+08
1e+09
Td

Fig. 18